Analyst

PAPER

View Article Online
View Journal | View Issue

Cite this: *Analyst*, 2015, **140**, 6313

Lipid-conjugated fluorescent pH sensors for monitoring pH changes in reconstituted membrane systems†

Gerdi Christine Kemmer,[a] Sidsel Ammitzbøll Bogh,[b] Michael Urban,[c] Michael G. Palmgren,[a] Tom Vosch,[b] Jürgen Schiller[d] and Thomas Günther Pomorski*[a]

Received 12th June 2015,
Accepted 10th August 2015

DOI: 10.1039/c5an01180a

www.rsc.org/analyst

Accurate real-time measurements of the dynamics of proton concentration gradients are crucial for detailed molecular studies of proton translocation by membrane-bound enzymes. To reduce complexity, these measurements are often carried out with purified, reconstituted enzyme systems. Yet the most paramount problem to detect pH changes in reconstituted systems is that soluble pH reporters leak out of the vesicle system during the reconstitution procedure. This requires loading of substantial amounts of pH-sensors into the lumen of unilamellar liposomes during reconstitution. Here, we report the synthesis and detailed characterisation of two lipid-linked pH sensors employing amine-reactive forms of semi-naphthorhodafluors (SNARF®-1 dye) and rhodamine probes (pHrodo™ Red dye). Lipid-conjugation of both dyes allowed for efficient detergent-based reconstitution of these pH indicators into liposomes. Vesicle-embedded pHrodo™ displayed excellent photostability and an optimal pH-response between 4 and 7. The suitability of the lipid-linked pHrodo™ probe as a pH reporter was demonstrated by assaying the activity of a plant plasma membrane H^+-ATPase (proton pump) reconstituted in proteoliposomes.

Introduction

Cells and organelles depend on electrochemical gradients across their membranes. Membrane-embedded biological pumps are key players in maintaining these gradients through primary active transport of ions, but the precise mechanisms underlying electrogenic transport are not yet completely understood. Among these pumps, plasma membrane H^+-ATPases couple ATP hydrolysis to H^+ transport out of the cell. In fungi and plants, they are essential for establishing and maintaining the crucial transmembrane electrochemical gradient of H^+, which provides the driving force for the uptake of nutrients and other cell constituents through an array of secondary transport systems.[1–4]

The study of H^+-translocating proteins at the molecular level is challenging due to the complexity of the membrane in which they are embedded. Thus, as an important step towards a detailed understanding of their action and molecular functioning, current studies focus on isolated organelles and on homogeneous preparations of membrane proteins reconstituted into an artificial lipid environment. The latter offers a well-defined experimental system where no unknown or unwanted proteins are present. Moreover, reconstituted systems allow for a more flexible choice of biochemical, biophysical and microscopy techniques for characterising the related proteins.[5] H^+ fluxes in these systems are typically followed indirectly by use of pH-sensitive dyes that change absorbance or fluorescence properties in response to the formation of pH gradients across the membrane.

Dyes such as pyranine (8-hydroxypyrene-1,3,6-trisulphonic acid) have been used to monitor the intravesicular pH values in mechanistic studies of H^+-translocating membrane-bound proteins.[6,7] However, the modest brightness of pyranine can be a drawback in fluorescence measurements and high concentrations (up to several millimoles) are required during

[a]*Centre for Membrane Pumps in Cells and Disease – PUMPKIN, Department of Plant Biology and Biotechnology, University of Copenhagen, Thorvaldsensvej 40, 1871 Frederiksberg C, Denmark. E-mail: tgp@plen.ku.dk*
[b]*Nano-Science Center, Department of Chemistry, University of Copenhagen, Universitetsparken 5, 2100 Copenhagen, Denmark*
[c]*Institute of Biochemistry, Biocenter, Goethe-University, Max-von-Laue-Str. 9, D-60438 Frankfurt, Germany*
[d]*Institute of Medical Physics and Biophysics, Faculty of Medicine, University of Leipzig, 04107 Leipzig, Germany*

†Electronic supplementary information (ESI) available: Scheme of SNARF conjugation to DOPE is shown (Fig. S1), head group lipid composition of lecithin is demonstrated (Fig. S2), fluorescence emission spectra of soluble SNARF in buffer solutions of different pH are presented (Fig. S3), size distribution of liposomes containing pH-sensors (Fig. S4), comparison of relative fluorescence change Pyranine and pHrodo-DOPE (Fig. S5), and conversion of fluorescent intensity changes to pH changes is described (Fig. S6). See DOI: 10.1039/c5an01180a

reconstitution. A number of alternative pH-sensitive dyes with improved brightness and photostability are available, such as seminaphthorhodafluors (SNARFs) and rhodamine-based pHrodo dyes, allowing their application in fluorescence microscopy and flow cytometry from the single vesicle down to the single molecule level.[8–12] Yet the most paramount problem of reconstituted systems is the loading of sufficient amounts of these fluorophores into unilamellar liposomes (diameter 40–400 nm). Most protein reconstitution methods include a detergent removal step usually performed either by dilution, dialysis, or the use of detergent absorbing hydrophobic polystyrene beads.[5,13] This procedure typically results in a significant loss of the dye from the liposomal lumen.[14]

In this study, we circumvented this problem by covalently linking the pH-sensing fluorophore to a membrane phospholipid *via* an amide bond. Two different pH-sensitive fluorophores, SNARF (SNARF®-1 carboxylic acid, acetate, succinimidyl ester) and pHrodo (pHrodo™ Red, succinimidyl ester) were linked to dioleoylphosphatidylethanolamine (DOPE) by conjugation to the ethanolamine head group. The corresponding lipid-conjugated derivatives were characterised regarding pH dependence of their fluorescence emission, their reconstitution efficiency and applicability for monitoring pH changes in reconstituted liposomal systems.

Experimental

Materials

DOPE and dioleoylphosphatidylcholine (DOPC) were purchased from Avanti Polar Lipids (Alabaster, AL, USA). Soybean lecithin (Type II-S, 14–23% choline basis) was purchased from Sigma-Aldrich (Brøndby, Denmark). Reactive pH-sensor esters of pHrodo (pHrodo™ Red, succinimidyl ester) and SNARF (SNARF®-1 carboxylic acid, acetate, succinimidyl ester), as well as water-soluble pH sensors 5-(and-6)-carboxy SNARF®-1 and pHrodo® Red Dextran (10 000 MW) were purchased from Invitrogen (Eugene, OR, USA). The detergent *n*-dodecyl-β-D-maltoside (DDM) was obtained from Glycon Biochemicals (Luckenwalde, Germany). Bio-beads SM-2 (Bio-Rad Laboratories, Hercules, CA) were washed in methanol and rinsed with double-distilled water before use. Ultrapure water was obtained from an in-house Millipore water purification system (Merck KGaA, Darmstadt, Germany). Unless indicated otherwise, all other chemicals and reagents were obtained from Sigma-Aldrich (Brøndby, Denmark).

Synthesis and purification of the lipid-conjugated pH-sensors

DOPE (1 mg; 1.35 μmol) in chloroform was evaporated to dryness under a stream of nitrogen and re-suspended in 60 μL anhydrous methanol containing trimethylamine (1.14 μmol). After addition of the pH-sensor ester reagent (1 mg; 1.6 μmol) in anhydrous methanol (60 μL), the reaction mixture was stirred for 1 h at room temperature. Any remaining pH-sensor ester reagent was hydrolysed over 30 min by the addition of water (1 mL). Afterwards, lipids were extracted from the reaction solution according to Bligh and Dyer.[15] The lipid extracts were applied onto normal phase silica gel thin layer chromatography plates (TLC, silica gel 60 F254, Merck) and developed with a mixture of 90/54/7 (v/v/v) of chloroform, methanol, and 25% aqueous ammonium hydroxide. The band containing the product was scraped off and extracted using a mixture of chloroform, methanol, and water (1/2.2/1, by volume). This extract was further purified on a second TLC plate which was developed with a mixture of 50/20/10/10/2.5 (v/v/v/v/v) chloroform, acetone, methanol, glacial acetic acid, and water. The band containing the product was scraped off and extracted as described above. The successful labelling of DOPE was confirmed by matrix-assisted laser desorption ionisation time-of-flight mass spectrometry (MALDI-TOF MS). Before photographing under ambient light or long-wave UV light TLC plates were dried completely to remove any remaining component from the mobile phase. To visualise DOPE, TLC plates were subsequently stained with primuline (0.005% in acetone/water, 8/2; v/v)[16] and photographed under long-wave UV light.

MALDI-TOF mass spectrometry

For the acquisition of positive or negative ion mass spectra, 0.5 M DHB in methanol or 10 mg mL^{-1} 9-aminoacridine (9-AA) in isopropanol/acetonitrile (60/40, v/v) were used as matrices, respectively.[17,18] As the quality of the spectra recorded in the presence of 9-AA depends significantly on the applied solvent system, the applied lipid extracts were diluted with isopropanol/acetonitrile (60/40, v/v).[19] All samples were pre-mixed with the matrix prior to deposition onto the MALDI target. All MALDI-TOF mass spectra were acquired on a Bruker Autoflex mass spectrometer (Bruker Daltonics, Bremen, Germany). The system utilises a pulsed nitrogen laser, emitting at 337 nm. The extraction voltage was 20 kV and gated matrix suppression was applied to prevent the saturation of the detector by matrix ions.[20] For each mass spectrum, 128 single laser shots were averaged. The laser fluence was kept about 10% above threshold (*i.e.* the minimum laser fluence required to achieve detectable signals) to obtain optimum signal-to-noise (S/N) ratios. In order to enhance the spectral resolution all spectra were acquired in the reflector mode using delayed extraction conditions. More detailed methodological descriptions of MALDI-TOF-MS are available in Fuchs.[21]

Liposome preparation

Liposomes were prepared by manual extrusion. Briefly, chloroform stocks of soybean lecithin (10 mg, ~11.5 μmol) and lipid-linked pH-sensor (60 nmol for SNARF-DOPE; 20 nmol for pHrodo-DOPE) were dispensed into a round bottom flask, mixed and dried by rotary evaporation, followed by incubation for 1 h under vacuum (30 mbar) at room temperature. The lipid film was rehydrated in 667 μL of reconstitution buffer (10 mM Mes-KOH, pH 6.5, 50 mM K_2SO_4, 20% glycerol) by vortexing in the presence of a glass pearl, and passed 41 times through 0.2 μm size nucleopore polycarbonate membranes (Nuclepore™, Whatman GmbH, Germany) mounted in a mini-

extruder (Avanti Polar Lipids, Alabaster, AL). The resulting liposomes were kept at 4 °C and used within 1 week.

pH titration of lipid-conjugated pH-sensors

For assessment of the pH-dependence of DOPE-conjugated pH-sensors, a range of different buffers between pH 2.5 and 10.7 were prepared. Each buffer component was prepared as 20 mM stock supplemented with 52.5 mM K_2SO_4 and the individual buffer components were mixed to obtain the required pH values. Citrate/phosphate buffer was used for pH 2.5–7, phosphate buffer for pH 7–8, and carbonate/bicarbonate buffer for pH 9–10.7. Water-soluble SNARF and pHrodo dextran were used at 0.5 μM, and 3–12 μg mL^{-1}, respectively. Prior to fluorescence measurements, liposomes containing the DOPE-conjugated pH-sensors were diluted 1 : 200 in the respective pH-buffers supplemented with the K^+ ionophore valinomycin (62.5 nM) and the protonophore carbonyl cyanide *m*-chlorophenylhydrazone (CCCP, 5 μM) for at least 15 min to allow equilibration of pH values between the inside and the outside of the liposomes. The presence of the K^+ ionophore valinomycin and high concentrations of K^+ inside and outside the vesicles prevent the build-up of a membrane voltage difference. For each buffer condition a fluorescence emission spectrum was recorded with a Fluoromax-4 spectrofluorometer (Horiba, Edison, NJ, USA) equipped with a LFI-3751 temperature controller (Wavelength Electronics, Bozeman, MT, USA) at 25 °C. Spectra were corrected using fluorophore-free liposomes at equal concentration and pH. SNARF was excited at 543 nm, and fluorescence recorded between 560 and 750 nm. For calibration curves, the ratio of intensities of low-wavelength maximum (at 580 nm) and the high-wavelength maximum (at 630 nm for soluble SNARF, and 650 nm for SNARF-DOPE) was calculated. The pHrodo dye was excited at 532 nm and emission recorded between 550 and 700 nm; the maximum for each pH was extracted and normalised to the maximum at pH 3. For all calibration curves, data (ratio of intensities and normalised maximum intensity for SNARF and pHrodo, respectively) was fitted using the built-in Boltzmann function of Origin (OriginLab, Northampton, MA).

Photophysical characterisation of DOPE-conjugated pHrodo

Liposomes (30 μL; 125 nmol of lipid) with pHrodo-DOPE were diluted in 2.7 mL transport buffer (20 mM MOPS-KOH, pH 7.0, 52.5 mM K_2SO_4) with the pH value adjusted by addition of HCl. Absorption spectra were measured on a Lambda 1050 (PerkinElmer) with 2 nm slits and were corrected for scattered light by subtracting an absorption spectrum of a dye free sample. For the emission measurements pHrodo-DOPE and the reference dye were excited with a 509 nm pulsed laser with a laser power of 190 μW (model number P-C-510 PicoQuant GmbH) on a Fluotime 300 instrument (PicoQuant GmbH). All emission spectra were measured with a pulse repetition rate of 40 MHz and were corrected for the spectral response of the detector. Slit widths of 5 nm were used for all emission measurements. Time-correlated single photon counting experiments were conducted with the same 509 nm pulsed laser on a Fluotime 300 instrument. The pulse rate was 16 MHz and the emission was measured at 590 nm. Measurements were performed at 25 °C in a water thermostated cuvette holder. The fluorescence decays were fitted to a bi-exponential function. The full width at half-maximum (FWHM) of the instrument response function was typically in the order of 42 ps.

Preparation of plasma membrane H^+-ATPase isoform 2 (AHA2)

A 73 amino acid C-terminal truncated version of the protein (aha2Δ73), containing a hexahistidine (6 × His) tag at the N-terminal end of the protein, was overexpressed in *Saccharomyces cerevisiae* strain RS-72.[22] The cells were lysed by vortexing with glass beads, and the protein was solubilised and purified with DDM at a ratio of 3/1 detergent/protein (w/w) using batch-binding to a Ni^{2+}-NTA resin. The purified protein was finally concentrated to 5–10 mg mL^{-1} using centrifugal concentrators with a cut-off at 30 kDa (Vivaspin 20, GE Healthcare), frozen in liquid nitrogen and stored at −80 °C in storage buffer containing 50 mM Mes-KOH (pH 7), 50 mM KCl, and 20% (v/v) glycerol until further use.

Vesicle reconstitution and analysis

Purified H^+-ATPase was reconstituted into preformed liposomes as described[22] using 75 μg purified protein per reconstitution. In short, preformed liposomes (156 μL of ~11 μmol phospholipid per mL), purified protein (typically 10 μL of 7.5 mg mL^{-1}), and detergent (octyl β-D-glucopyranoside, 50 mM final concentration) were mixed in a final volume of 220 μL reconstitution buffer. Pyranine (8-hydroxypyrene-1,3,6-trisulfonic acid) was added at this step to 25 mM final concentration when indicated. The solubilised protein/lipid/detergent mixture was applied to a gel-filtration column (Sephadex G-50 Fine, 2 mL packed in 2 mL disposable syringes) and incubated for 5 min before centrifugation (180*g*, 7 min). The eluate was incubated for 30 min at room temperature with 100 mg of wet bio-beads under overhead rotation to eliminate traces of detergent. Protein-free liposomes were prepared similarly by replacing purified protein with reconstitution buffer.

Phospholipid vesicle recovery after detergent removal was determined by measuring the amount of phospholipid phosphorus[23] before and after reconstitution. The concentrations of the DOPE-conjugated pH-sensors and pyranine before and after reconstitution into liposomes were quantified fluorimetrically (*vide supra*); comparison between these two numbers yielded the sensor recovery. The size of the vesicles was characterised *via* nanoparticle tracking (NanoSight LM14, Nanosight Ltd.); typical diameters for extruded liposomes and reconstituted liposomes were 134 ± 45 and 109 ± 31 nm, respectively.

H^+ transport measurement

To determine H^+ pumping activity, proteoliposomes (5 μL) were added to 1 mL transport buffer (20 mM MOPS-KOH, pH 7.0, 52.5 mM K_2SO_4) containing 62.5 nM valinomycin, and equilibrated for 15–30 min. During measurements, 2 mM ATP/ATP-analogue (buffered at pH 7) was added and H^+ pumping was initiated by the addition of $MgSO_4$ (3 mM final concen-

tration), and when indicated dissipated by the addition of 5 μM CCCP. The non-hydrolysable ATP-analogue adenyl-5′-yl imidodiphosphate (AMP-PNP) was used as a control in the same concentration as ATP. Fluorescence traces were recorded for 600 s at 25 °C by a Fluoromax-4 spectrofluorometer at the following settings: 532 nm excitation, 585 nm emission, 3 nm slit widths, 0.1 s resolution (pHrodo) and 460 nm excitation, 1 nm slit width, 515 nm emission, 2 nm slit width, 0.1 s resolution (pyranine).

Results and discussion

Synthesis and purification of lipid-conjugated fluorescent pH indicators

DOPE was labelled with amine-reactive succinimidyl (NHS) esters of SNARF and pHrodo dyes under mild basic conditions using trimethylamine in methanol. The products were extracted and purified by two subsequent TLC runs. TLC analysis of the SNARF labelling reaction revealed multiple fluorescent bands (Fig. 1A and B). Under the reaction conditions used, the SNARF-NHS ester reacts readily with the amino group of DOPE yielding SNARF-DOPE; however, the aryl acetyl group was removed due to the known susceptibility of aryl acetates toward bases (Fig. 1C; ESI, Fig. S1†). DOPE-conjugated SNARF appeared as a pink band under ambient light with R_f values of 0.9 and 0.5 using alkaline and acidic TLC conditions, respectively. The positive ion MALDI-TOF mass spectrum of the purified product showed three signals in the high mass range (Fig. 1C). These peaks at m/z 1179.6 ($+H^+$), m/z 1201.5 ($+Na^+$), and m/z 1223.5 ($-H^+ + 2Na^+$) correspond exactly to the expected molecular weight of SNARF-DOPE. The peak at m/z 727.0 is characteristic for the DHB matrix cluster ion generated in the gas phase,[25] while the small peaks at m/z 774.1 and 795.1 could not be assigned. Free, unmodified DOPE (expected at m/z 744.5, 766.5 and 788.5) and free SNARF derivatives were not detectable, demonstrating efficient purification. There were furthermore indications that radical cations are generated in addition to commonly generated ion adducts: this is obvious from the unusual peak patterns (*cf.* the insert in Fig. 1C) and applies particularly to the peaks corresponding to the sodiated ions. A more detailed elucidation of these aspects, however, is beyond the scope of this publication.

TLC analysis of the pHrodo labelling reaction revealed a main band (intense pink under day light) with R_f values of 0.99 and 0.3 using alkaline and acidic TLC conditions, respectively (Fig. 1D and E). There were only minor by-products as assessed by some additional bands with low intensity, detectable under ambient and UV light. The positive ion mass spectrum of the purified product gave two peaks at m/z 1270.8

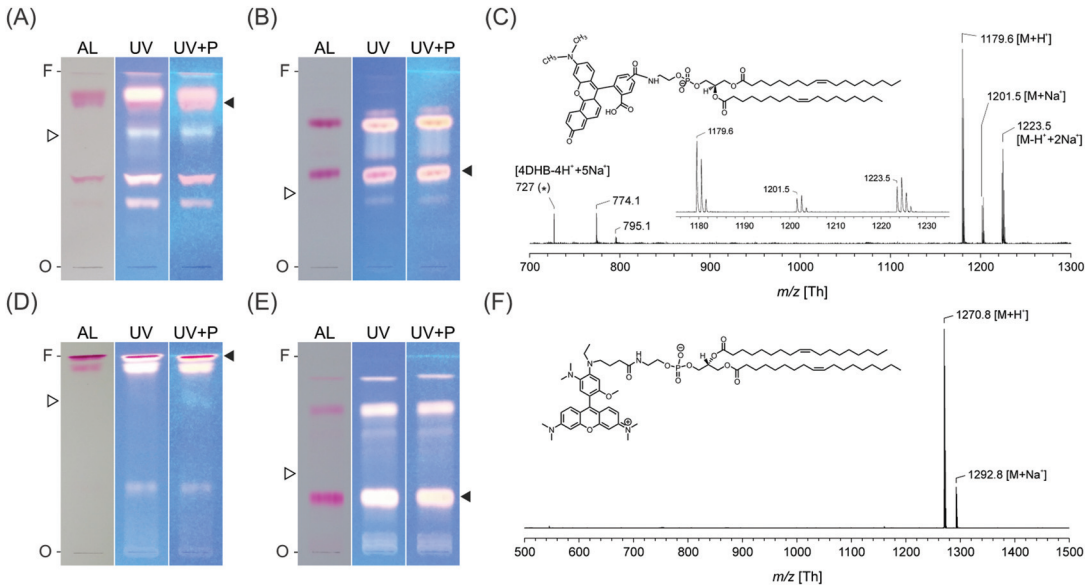

Fig. 1 Purification of lipid-conjugated pH-sensors. SNARF®-1 carboxylic acid, acetate, NHS ester (upper panel, A–C) or pHrodo Red NHS ester (lower panel, D–F) was reacted with DOPE and the resulting derivatives were extracted and resolved by alkaline TLC (A and D, respectively). After extraction of the indicated region (filled arrowhead in A and D), the samples were resolved by acidic TLC (B and E, respectively), and the indicated region (filled arrowhead in B, resp. E) was extracted as final product. See Experimental for the composition of the used solvent systems. Chromatograms shown were dried completely before photographing under ambient light (AL) or UV light before (UV) and after staining with primuline (UV + P). The position of non-reacted DOPE is indicated by an open arrowhead. O, origin; F, solvent front, of the chromatograms. The final products were analysed by MALDI MS (C and F, positive ion mode). For lipid-conjugated SNARF (C), the annotated peaks correspond to the proton (m/z 1179.6), the sodium (m/z 1201.5), and $H^+ + 2\ Na^+$ (m/z 1223.5) adducts (insets: chemical structure of SNARF-DOPE and expanded section of the chromatogram). The characteristic matrix peak is indicated by an asterisk. For lipid-conjugated pHrodo (F), the annotated peaks correspond to the proton and the sodium adducts (m/z 1270.8 and m/z 1292.8, respectively) (inset: chemical structure of pHrodo-DOPE; for pHrodo the chemical structure proposed by Ogawa[24] was used).

and 1292.8 (Fig. 1F) corresponding to the proton and sodium adducts of pHrodo-DOPE. No unreacted DOPE (expected at *m*/*z* 744.5, 766.5, and 788.5) or other products were detectable. Thus, the purity of the product is close to 100%.

pH-Dependence of lipid-conjugated fluorescent pH indicators

The lipid-conjugated pH-indicators were next characterised with respect to their fluorescence dependence on the buffer pH. These experiments were carried out following embedment of the probes in liposome prepared from soybean lecithin, a phospholipid mixture containing mainly phosphatidylcholine, -ethanolamine, -inositol and phosphatidic acid (ESI, Fig. S2†). Spectra of liposome-embedded, DOPE-conjugated SNARF exhibited two maxima, at 585 nm and 650 nm, and an apparent isosbestic point at 640 nm (Fig. 2A). The isosbestic point and the higher maximum were shifted towards higher wavelengths compared to water-soluble SNARF (600 nm and 630 nm, respectively; ESI, Fig. S3†). These values and pH-dependent fluorescence spectra of free SNARF are in line with previously published results.[26] As compared to water-soluble SNARF (pK_a = 6.7), the pH dependence of the lipid-conjugated form was shifted drastically to higher pK_a = 9.3 (Fig. 2B).

Results for vesicle-embedded pHrodo-DOPE in buffer solutions of different pH values are shown in Fig. 2C and D. The amplitude of fluorescence emission was strongly pH-dependent, and increased as the pH was lowered, whereas the overall shape of the spectrum was pH-independent (Fig. 2C). The conjugation to DOPE had a strong effect on the calibration curve of pHrodo (Fig. 2D), but not on the overall shape of the spectra (Fig. 2C). For dextran-linked, water-soluble pHrodo no pK_a is given by the manufacturer, but a log EC_{50} of 6.8 is specified which is in line with our data (pK_a = 6.9). For vesicle-embedded pHrodo-DOPE, the pK_a value was shifted to 5.6. It should be noted, however, that the fluorescence properties of both dyes are dependent on the local environmental conditions.[27] For example, when embedded into pure DOPC liposomes pHrodo-DOPE exhibited a pK_a of 4.5 (data not shown). Thus, careful controls are required to ensure that changes in the fluorescence signal are caused by pH changes as opposed to changes in the structure of the phospholipid bilayer (which

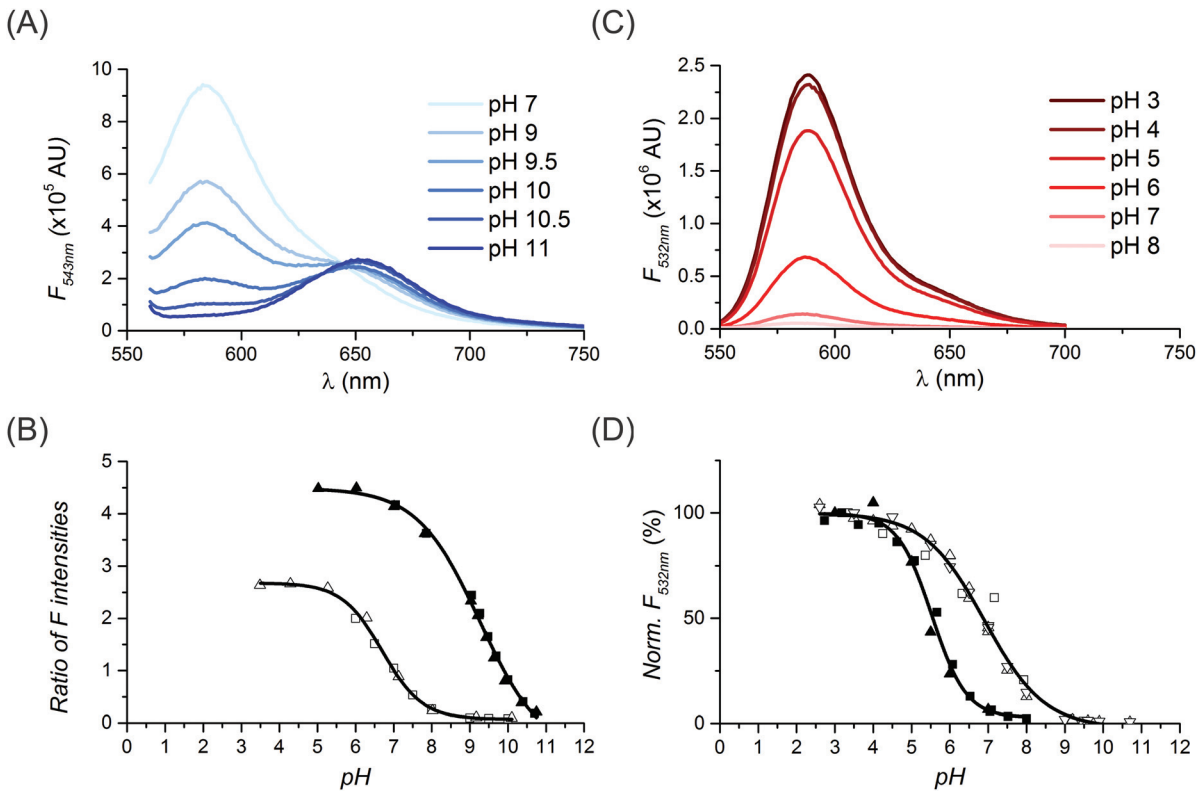

Fig. 2 pH-Dependence of SNARF and pHrodo fluorescence. Fluorescence emission spectra of vesicle-embedded SNARF- (A) and pHrodo-DOPE (C) in buffer solutions of different pH upon excitation at 543 and 532 nm, respectively. All measurements were performed in pH-adjusted buffers of the indicated pH values containing the protonophore CCCP (5 μM) and the K^+-ionophore valinomycin (62.5 nM) to equilibrate the pH between the inside and outside of the liposomes. Each spectrum represents an aliquot of a liposome stock solution diluted in buffer and incubated for at least 15 min. (B) Ratio of the fluorescence intensities derived from the respective fluorescence spectrum of vesicle-embedded SNARF-DOPE (solid symbols, 2 data sets) and water-soluble SNARF (open symbols, 2 data sets) as a function of pH. (D) pH-calibration curve of vesicle-embedded pHrodo-DOPE (solid symbols, 2 data sets) and water-soluble pHrodo (open symbols, 3 data sets). Different symbols denote independent experiments; lines represent global nonlinear least squares fit to the Boltzmann function. Norm. F, max fluorescence intensity for each pH was normalised to the maximum at pH 3.

Table 1 Recovery of lipid-conjugated pH-sensors compared to water-soluble pyranine after reconstitution. Relative recovery values of total lipid and pH-sensors, determined by phospholipid phosphorus measurement, and fluorescent spectroscopy, respectively. Normalised recovery given as ratio of fluorescence over total lipid recovery

	Total lipid (%)	Fluorescence (%)	Norm. recovery (%)
SNARF-DOPE	68 ± 29	70 ± 35	102 ± 3
pHrodo-DOPE	67 ± 10	70 ± 11	105 ± 14
Pyranine	77 ± 7	0.7 ± 0.2	0.9 ± 0.2

Results are the means ± SD of two, eight, and three independent reconstitutions with SNARF-DOPE, pHrodo-DOPE, and pyranine, respectively.

might be caused by altered lipid–ion interactions[28]). In the case of H^+-translocating ATPases, suitable controls are the use of non-hydrolysable ATP analogues (*vide infra*) or specific ATPase inhibitors.

Reconstitution of the lipid-conjugated pH indicators

To demonstrate the usefulness of lipid-conjugation for reconstitution, we determined the recovery of SNARF-DOPE and pHrodo-DOPE after a classical reconstitution procedure.[5,14,29] Liposomes doped with lipid-conjugated fluorescent pH indicators were destabilised using detergent and reconstituted by detergent removal based on Sephadex G-50 gel filtration and subsequent Bio-Bead treatment. Under these conditions, about 70–80% of the liposomes were recovered without significant loss of the lipid-conjugated fluorescent pH indicators (Table 1). Furthermore, the integrity of formed liposomes was confirmed by nanoparticle tracking (ESI, Fig. S4†). Thus, lipid-conjugation of pHrodo and SNARF allows for efficient reconstitution of these pH indicators into well-formed liposomes. By contrast, pyranine, a water-soluble pH-indicator added during reconstitution, was predominantly lost (recovery about 1%) during reconstitution.

Photophysical characterisation of lipid-conjugated pHrodo

Because vesicle-embedded pHrodo-DOPE displayed an excellent pH-response in the most interesting range between 4 and 7, we characterised this probe in more detail. Table 2 summarises the maximum absorption and emission wavelengths, fluorescence decay times and the estimated fluorescence quantum yield as a function of pH. The fluorescence quantum yields should only be treated as rough estimates due to significant scattering of the liposomes. Within the tested pH range (pH 5–7) the maximum absorption and emission wavelengths remained nearly unchanged around a value of 562 ± 3 nm and 590 nm, respectively; while the fluorescence quantum yield was found to decrease at higher pH. Using time-correlated single photon counting, the fluorescence decays of vesicle-embedded pHrodo-DOPE were recorded at different pH. The data was fitted with a bi-exponential function suggesting that two decay time components are present for pHrodo-DOPE in the vesicles. Though there were variations in the actual value of the two decay time components at different pH values, the intensity weighted average decay time τ_{int} only displayed minor changes. This limited change in the overall fluorescence decay time and the fact that the absorption spectrum remains nearly constant over the probed pH range, combined with the pH dependent fluorescence quantum yield, indicate that the pH dependent fluorescence response could be due to photo-induced electron transfer from the amine group.[32] Long-time excitation of vesicle-embedded pHrodo-DOPE (pulsed laser at 509 nm and 190 μW for 20 h at pH 6.8) caused no significant decrease in fluorescence (data not shown), demonstrating the excellent photostability of the sensor system.

Monitoring H^+ pumping by reconstituted H^+-ATPase using lipid-conjugated pHrodo

Next, the suitability of pHrodo-DOPE to monitor pH changes in reconstituted liposomal systems was tested. Purified and reconstituted *Arabidopsis thaliana* autoinhibited plasma membrane H^+-ATPase (AHA2) was used as a model transporter. It functions as an ATP-driven membrane intrinsic protein that plays a key role in the physiology of plants by controlling essential functions such as nutrient uptake and intracellular pH regulation.[4,33] Proteoliposomes with reconstituted plasma membrane H^+-ATPase were added to ATP-containing buffer (pH 6.8), and the fluorescence intensity monitored at 585 nm. At pH 6.8, lipid-linked pHrodo is weakly fluorescent but elicits a bright, red-fluorescent signal as the pH decreases locally, *i.e.* at an elevated H^+ concentration inside vesicles. Thus, despite the presence of lipid-conjugated fluorescent pH sensors on

Table 2 Photophysical properties of lipid-conjugated pHrodo. Absorption (λ_{abs}) and emission maxima (λ_{em}) in nm, fluorescence decay time components (τ_n) in ns and their relative amplitudes in %, the intensity weighted average decay time τ_{int} in ns, the χ^2 value of the fit and the estimated fluorescence quantum (Φ_{fl}) yield in % of pHrodo-DOPE containing soybean phosphatidylcholine vesicles in buffer solutions of different pH values

pH	λ_{max} (abs)	λ_{max} (em)	τ_1 (ns)/amplitude (%)	τ_2 (ns)/amplitude (%)	τ_{int} (ns)	χ^2	Est. Φ_{fl}[a] (%)
4.4	565	590	3.21/66.2	1.74/33.8	2.89	1.22	34
5.6	563	590	3.15/62.7	1.56/37.3	2.79	1.20	32
6.2	561	590	3.02/65.9	1.23/34.1	2.71	1.26	18
6.8	559	590	2.93/62.6	1.01/37.4	2.61	1.33	11

[a] The fluorescence quantum yield was determined by a relative method[30] using Rhodamine 6G (Φ_{fl} = 0.95 in absolute ethanol) as a standard,[31] and should only be treated as rough estimates due to significant scattering of the liposomes in the sample.

both vesicle leaflets, a decrease in vesicular lumen pH by the H^+-pump activity can be recorded.

To initiate H^+ pumping, Mg^{2+} was injected as the ATPase substrate is Mg^{2+}-ATP (Fig. 3A). Only H^+-ATPases oriented with their catalytic core domain towards the buffer medium are able to pump H^+ into the vesicle lumen and contribute to its acidification, which is monitored in this assay. All measurements were performed in the presence of the ionophore valinomycin to ensure that K^+-ions were free to diffuse out of the proteoliposomes in response to H^+ loading (Fig. 3A). These settings prevented the formation of a membrane potential, thereby eliminating any contribution from an inside positive electrical potential working against H^+ pumping. A representative trace of H^+-pump activity measured with pHrodo-DOPE is shown in Fig. 3B. In the presence of Mg^{2+}-ATP an increase in the fluorescence intensity of pHrodo-DOPE was observed, corresponding to the acidification of the internal volume of the liposomes (Fig. 3B, red trace). The addition of the protonophore CCCP abolished this effect, confirming the active H^+ transport into the proteoliposomes.

To further validate whether the changes in fluorescence were caused by H^+ pumping, empty liposomes and the non-hydrolysable ATP analogue AMP-PNP were included as controls in the transport assays. Incubation of empty liposomes with Mg^{2+}-ATP resulted in a minor nonspecific decrease in fluorescence (Fig. 3B, black trace) upon addition. The minor nonspecific decrease in fluorescence was also observed for both empty and protein-containing vesicles when AMP-PNP was used instead of ATP (Fig. 3D, black and red trace, respectively), which might be caused by altered lipid–ion interactions.[28] Collectively, these results demonstrate that pHrodo-DOPE is suitable for monitoring protein-mediated and ATP-fuelled pumping of H^+ against their concentration gradient into the vesicle lumen. A comparison of the relative changes in fluorescence of pHrodo-DOPE and pyranine showed a fluorescence decrease of 34% for pyranine and a fluorescence increase of 63% for pHrodo-DOPE (ESI, Fig. S5†), demonstrating the advantage of the novel pHrodo-DOPE. Detecting increasing instead of decreasing fluorescence intensity is furthermore desirable to avoid problems arising from photobleaching.

Finally, the fluorescence change was converted to the corresponding pH shift by correcting for the contribution of pH-sensors located on the outer monolayer and solving the Boltzmann function for pH as described in the ESI.† H^+ pumping buffer pH in the presence of ATP was 6.78 and was lowered to 6.16 upon activation of the H^+ pump in the trace shown here (Fig. 4). On average (n = 7), the resulting ΔpH upon activation of the H^+-pump was 0.53, ranging from 0.3 to 0.74, with a standard deviation of 0.16. This is small compared to published data (ΔpH > 2) for proton pumps *in planta*,[4] and is most likely a result of passive leakage of H^+ through the artificial liposome membrane.

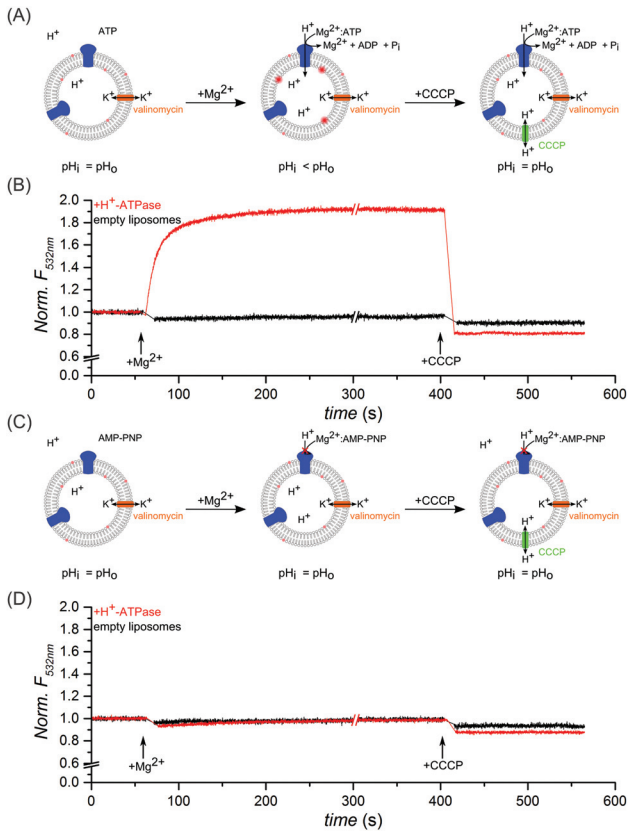

Fig. 3 Monitoring H^+ pumping by reconstituted H^+-ATPase using lipid-conjugated pHrodo. (A) Illustration of the transport assay on proteoliposomes with reconstituted H^+-ATPase. Addition of Mg^{2+} to ATP-containing buffer initiated ATP hydrolysis and H^+ pumping into the vesicle lumen. Valinomycin was always present to mediate K^+ exchange and prevent the build-up of a transmembrane electrical potential. After reaching saturation conditions the H^+ gradient was disrupted by the addition of CCCP. Breaks in the traces denote intervals omitted for comprehensiveness. (B) Fluorescence changes for proteoliposomes (red) compared to empty liposomes (black) in the presence of ATP and Mg^{2+}. For quantification of the changes in the vesicular pH see ESI, Fig. S6.† (C) Illustration of a control experiment carried out in presence of AMP-PNP, a non-hydrolysable analogue of ATP. (D) Fluorescence changes for proteoliposomes (red) compared to empty liposomes (black) in the presence of AMP-PNP and Mg^{2+}. For clarity, ATP/ATP-analogue additions were omitted in panel (B) and (D).

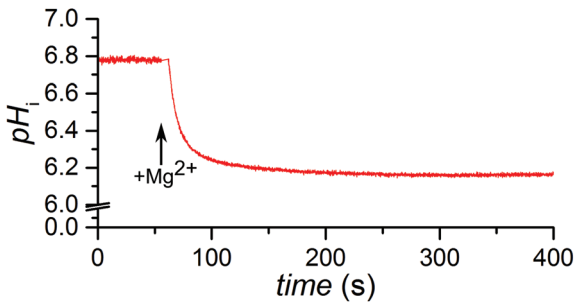

Fig. 4 pH-gradient generated by reconstituted H^+-ATPase. The H^+-pump activity trace for proteoliposomes from Fig. 3A was converted into pH_i units (pH measured by fluorophores on the inside membrane monolayer only) as described in ESI.†

Conclusions

In this study we describe the synthesis of two lipid-linked pH sensors, and demonstrate their application to monitor pH changes in reconstituted liposomal systems. The major advantage of this approach is that the lipid-linked pH sensors efficiently co-reconstitute with membrane proteins into liposomes, thereby avoiding their loss during reconstitution. This approach facilitates the study of H^+ translocation by membrane-bound enzymes, as exemplified by the analysis of a model plant proton pump employing lipid-conjugated pHrodo. The excellent photostability of the pHrodo probe might be helpful in future single vesicle studies. Lipid-conjugated SNARF (pK_a 9.3) can be useful for studies in which cation transport by ATPases is associated with H^+ counter-transport, *e.g.* in case of Na^+-translocating ATPases.[34,35] Furthermore, the system described in this work has the significant benefit of detecting the pH (and ions such as Mg^{2+}) close to the membrane bilayer which can be exploited for the development of sensor systems in biotechnology.[36]

In conclusion, both synthesised lipid-conjugated pH sensors open up for a wide range of biophysical and biological applications.

Acknowledgements

We are grateful to Anne-Mette Bjerg Petersen for excellent technical assistance. This work was supported by the Danish Council for Independent Research | Natural Sciences (FNU, grant number 1323-00297), the Research Centre 'bioSYNergy' funded by the UCPH Excellence Programme for Interdisciplinary Research, the Villum Foundation (Project number VKR023115) and the Danish National Research Foundation through the PUMPKIN Centre of Excellence (DNRF85).

Notes and references

1 J. C. Meade, C. L. Li, J. K. Stiles, M. E. Moate, J. I. Penny, S. Krishna and R. W. Finley, *Parasitol. Int.*, 2000, **49**, 309–320.
2 R. K. Nakamoto and C. W. Slayman, *J. Bioenerg. Biomembr.*, 1989, **21**, 621–632.
3 C. L. Slayman, W. S. Long and C. Y. H. Lu, *J. Membr. Biol.*, 1973, **14**, 305–338.
4 M. G. Palmgren, *Annu. Rev. Plant Physiol.*, 2001, **52**, 817–845.
5 J. L. Rigaud and D. Levy, *Liposomes, Pt B*, 2003, **372**, 65–86.
6 N. R. Clement and J. M. Gould, *Biochemistry*, 1981, **20**, 1534–1538.
7 A. Holoubek, J. Večeř and K. Sigler, *J. Fluoresc.*, 2007, **17**, 201–213.
8 S. Brasselet and W. E. Moerner, *Single Mol.*, 2000, **1**, 17–23.
9 J. Y. Han and K. Burgess, *Chem. Rev.*, 2010, **110**, 2709–2728.
10 R. Watanabe, K. V. Tabata, R. Iino, H. Ueno, M. Iwamoto, S. Oiki and H. Noji, *Nat. Commun.*, 2013, **4**, 1631.
11 Y. Fu, M. M. Collinson and D. A. Higgins, *J. Am. Chem. Soc.*, 2004, **126**, 13838–13844.
12 X. Shi, J. Lim and T. Ha, *Anal. Chem.*, 2010, **82**, 6132–6138.
13 R. Schubert, *Liposomes, Pt A*, 2003, **367**, 46–70.
14 T. Leiding, K. Górecki, T. Kjellman, S. A. Vinogradov, C. Hägerhäll and S. P. Årsköld, *Anal. Biochem.*, 2009, **388**, 296–305.
15 E. G. Bligh and W. J. Dyer, *Can. J. Biochem. Physiol.*, 1959, **37**, 911–917.
16 T. White, S. Bursten, D. Federighi, R. A. Lewis and E. Nudelman, *Anal. Biochem.*, 1998, **258**, 109–117.
17 J. Schiller, J. Arnhold, S. Benard, M. Müller, S. Reichl and K. Arnold, *Anal. Biochem.*, 1999, **267**, 46–56.
18 G. Sun, K. Yang, Z. Zhao, S. Guan, X. Han and R. W. Gross, *Anal. Chem.*, 2008, **80**, 7576–7585.
19 B. Fuchs, A. Bischoff, R. Süß, K. Teuber, M. Schürenberg, D. Suckau and J. Schiller, *Anal. Bioanal. Chem.*, 2009, **395**, 2479–2487.
20 M. Petković, J. Schiller, M. Müller, S. Benard, S. Reichl, K. Arnold and J. Arnhold, *Anal. Biochem.*, 2001, **289**, 202–216.
21 B. Fuchs, R. Süß and J. Schiller, *Prog. Lipid Res.*, 2010, **49**, 450–475.
22 F. C. Lanfermeijer, K. Venema and M. G. Palmgren, *Protein Expression Purif.*, 1998, **12**, 29–37.
23 G. Rouser, S. Fleische and A. Yamamoto, *Lipids*, 1970, **5**, 494–496.
24 M. Ogawa, N. Kosaka, C. A. Regino, M. Mitsunaga, P. L. Choyke and H. Kobayashi, *Mol. BioSyst.*, 2010, **6**, 888–893.
25 J. Schiller, R. Süß, B. Fuchs, M. Müller, M. Petković, O. Zschörnig and H. Waschipky, *Eur. Biophys. J. Biophys.*, 2007, **36**, 517–527.
26 S. Bassnett, L. Reinisch and D. C. Beebe, *Am. J. Physiol.*, 1990, **258**, C171–C178.
27 I. D. Johnson, *Molecular Probes handbook, A guide to fluorescent probes and labeling technologies*, Life Technologies Corporation, 11th edition, 2010.
28 H. Binder and O. Zschornig, *Chem. Phys. Lipids*, 2002, **115**, 39–61.
29 J. L. Rigaud, D. Levy, G. Mosser and O. Lambert, *Eur. Biophys. J. Biophys.*, 1998, **27**, 305–319.
30 C. Würth, M. Grabolle, J. Pauli, M. Spieles and U. Resch-Genger, *Nat. Protocols*, 2013, **8**, 1535–1550.
31 D. Magde, R. Wong and P. G. Seybold, *Photochem. Photobiol.*, 2002, **75**, 327–334.
32 Q. A. Best, R. S. Xu, M. E. McCarroll, L. C. Wang and D. J. Dyer, *Org. Lett.*, 2010, **12**, 3219–3221.
33 R. Serrano, M. C. Kielland-Brandt and G. R. Fink, *Nature*, 1986, **319**, 689–693.
34 K. Soontharapirakkul and A. Incharoensakdi, *BMC Biochem.*, 2010, 11.
35 Y. V. Balnokin, L. G. Popova, L. Y. Pagis and I. M. Andreev, *Planta*, 2004, **219**, 332–337.
36 A. D. Robison, D. Huang, H. Jung and P. S. Cremer, *Biointerphases*, 2013, 8.

